Phase Behavior, Structure and Dynamical Arrest of Charged Nanoplatelets Covered With a Thermo-Responsive Shell

Imane Boucenna, Florent Carn, Ahmed Mourchid

▶ **To cite this version:**

Imane Boucenna, Florent Carn, Ahmed Mourchid. Phase Behavior, Structure and Dynamical Arrest of Charged Nanoplatelets Covered With a Thermo-Responsive Shell. Soft Matter, In press. hal-04677680

HAL Id: hal-04677680
https://hal.science/hal-04677680v1

Submitted on 26 Aug 2024

HAL is a multi-disciplinary open access archive for the deposit and dissemination of scientific research documents, whether they are published or not. The documents may come from teaching and research institutions in France or abroad, or from public or private research centers.

L'archive ouverte pluridisciplinaire **HAL**, est destinée au dépôt et à la diffusion de documents scientifiques de niveau recherche, publiés ou non, émanant des établissements d'enseignement et de recherche français ou étrangers, des laboratoires publics ou privés.

Phase Behavior, Structure and Dynamical Arrest of Charged Nanoplatelets Covered With a Thermo-Responsive Shell

Imane Boucenna, Florent Carn and Ahmed Mourchid*

Matière et Systèmes Complexes (MSC), UMR 7057 CNRS and Université Paris Cité
10 rue Alice Domon et Léonie Duquet, 75205 Paris Cedex 13, France

Key words: Liquid crystals, Nanoplatelets, Thermo-Responsive polymer, X-ray scattering, Rheology

Abstract

Nanoplatelets open up a wide range of possibilities for building macroscopic advanced materials with novel properties linked to their shape anisotropy. A challenge consists of controlling the order of positioning and orientation in three dimensions by assembly to exploit the collective properties at the macroscale. To date, most of the research effort has been focused on controlling the phase behavior of hard nanoplatelets. In this letter, we tackle the case of core/shell nanometric platelets, composed of an athermal mineral core (laponite clay) and a polymeric soft shell (triblock copolymer) whose conformation can be thermally modulated. The structural and mechanical investigations show that the behavior of these nanoplatelets allows the emergence of a non-birefringent phase, composed of random stacks of nanoplatelets, in a relatively low concentration range. The thermosensitive nature of the shell prompts a transition from random stacks to columnar stacks, associated with a steep increase of viscoelasticity and birefringence yielding highly viscoelastic birefringent suspensions. The sequence of these textures were recently predicted numerically, including in the ionic strength range of the phase diagram investigated here. Our results, based on an easy-to-implement process, open up a new route for controlling the assembly of nanoplatelets at the nanoparticle scale.

Two-dimensional nanoparticles (i.e. nanoplatelets) are used to self-assemble advanced macroscopic materials with novel properties linked to their platelet shape. This has recently been demonstrated in single-photon emitting devices [1], solar cells, electrode materials [2], solar concentrators [3] or photo-catalytic devices [4]. The new emerging applications based on collective properties indicates renewed interest in studying the phase behavior of nanoplatelets, with the aim of controlling the order of positioning and orientation of nanoplatelets in three dimensions by nanoparticle assembly [5-10].

To date, most of the research effort has been focused on controlling the phase behavior of hard nanoplatelets. However, many many questions remain open, both experimentally and theoretically, because when the shape anisotropy of the nanoparticle is in play, a very rich phase diagram akin to liquid crystalline-type phases is expected. For nanoplatelets, equilibrium isotropic (I) and nematic (N) phases were identified a long time ago [11]. The nematic phase exhibits a long-range orientational order but lack long-range positional order. However, it is only recently that experimental formation of mesophases with positional order in addition to orientation, such as the cubatic-like (CUB) and the columnar (C) structures, has been observed though these phases were predicted decades before by numeric simulation [12-16]. The pioneering theoretical investigation was carried out for hard nanoplatelets at 3 varying aspect ratios (thickness/diameter) of 0.1, 0.2 and 0.3. For aspects ratios between 0.2 and 0.3 the new CUB mesophase emerges instead of a N mesophase [17] whereas the occurrence of I/N/C phase transitions was detected for the smaller aspect ratio. The CUB mesophase consists of finite stacks of nanoplatelets, orthogonally oriented with respect to closest neighboring stack. The transition from I to CUB was described by the authors as a weakly first order phase transition because the nanoplatelets show a strong tendency to associate in short columns even in the dilute regime. Later on, other numerical studies have questioned the stability of the CUB mesophase, arguing that the CUB structure is a metastable glassy state in the I/C phase transformation [18]. From an experimental point of view, the identification of the CUB mesophase is a difficult task due to the absence of optical birefringence [13] and the need to use high resolution structural analysis techniques that are non-disruptive [6]. However, the appearance of the different liquid crystalline phases presented above (i.e. I/N/CUB/C) has been confirmed by a few experimental studies on hard nanometric platelets showing the particular aspect ratios previously identified in the numerical simulations [12-13]. Interestingly, the CUB mesophase has also recently been detected by magnetic resonance imaging

in millimeter-sized granular disks. [19] Beyond the CUB mesophase, the existence of new structures composed of alternating nematic-antinematic sheets has been predicted by recent numerical simulations that take into account the anisotropy of shape and anisotropy of the electrostatic interaction potential between the charged and infinitely thin platelets within the nonlinear Poisson-Boltzmann formalism [20, 21]. These textures, which to our knowledge have not yet been experimentally detected, are expected to appear in the isotropic region of the phase diagram near the I/N transition.

In the present study, we investigate for the first time the phase behavior, structure and rheology of suspensions of core/shell nanometric platelets composed of an athermal mineral core and a thermo-responsive soft shell. More precisely, we considered aqueous suspensions of polydisperse core/shell nanoplatelets composed of laponite RDS clay nanoparticles and a soft shell of pluronic copolymer F127 coated on them. Laponite is a synthetic smectite clay that can be considered as nanoplatelets having a thickness l = 9.2 Å and an average diameter d = 280 Å with a diameter polydispersity of 30 %. Electrostatic interactions between the nanoplatelets are screened due to the presence of a conterion, $Na_4P_2O_7$, which yield a Debye length comparable to the nanoparticle thickness. The addition of the conterions also ensures full thermalization of the aqueous suspensions because it screens the positive edge charges on the laponite platelets and then decreases their viscosity in aqueous dispersions when the concentration $\phi \leq 12$ wt. %. The pluronic copolymer, F127, coating the laponite particles is a triblock copolymer poly(ethylene oxide)/poly(propylene oxide)/poly(ethylene oxide), noted PEO-PPO-PEO. The thermo-sensitive nature of this macromolecule, in water solutions, is reflected in two successive processes mediated by temperature: (i) self-association of the most hydrophobic propylene oxide blocks, above a critical temperature, while the PEO stays in contact with water forming a shell that protects the PPO blocks; (ii) when the temperature increases further, there is an induced increase in size of the PEO brushes, yielding an effective volume fraction increase. Accordingly, when this copolymer is solely present in solution, it first micellizes at the critical micellization temperature and forms solidlike cubic phases above the gelation temperature [22, 23].

The block copolymer poly(ethylene oxide)-poly(propylene oxide)-poly(ethylene oxide), has a nominal weight average molar mass of 12600 g/mol (Sigma-Aldrich). The synthetic laponite RDS clay nanoparticles possess tetrasodium pyrophosphate counterions, $Na_4P_2O_7$, which screen the electrical charges and improve their complete dispersion and stability in aqueous solutions without

changing the structural behavior of the suspensions [24]. The amount of this counterion present in solution is in the form of ($4Na^+$, $P_2O_7^{4-}$) and yields us to estimate the ionic strength $I = \frac{1}{2}\sum_i c_i Z_i^2$ and thus the Debye length κ^{-1} = 7.8 Å at the laponite concentration of 9 wt. %, where c_i is the ion i molar concentration and Z_i is its valency. Likewise, the estimated Debye length at 3 wt. % is 13.4 Å. As a consequence, electrostatic interactions are screened for the concentrations investigated in this study.

Small angle X-ray scattering (SAXS) measurements were carried out at Synchrotron Soleil facility in France. The typical specifications of the experimental setup were: X photon energy = 12 keV, wavelength = 1.03 Å and sample-to-2d detector distance = 3.5 m. The scattering profiles on each sample, sealed in 1.5 mm quartz cell, were recorded at different temperatures, radially averaged and normalized by water scattering intensity to get intensities in absolute scale (cm^{-1}). The contribution of the nanoparticles to the scattering signal is predominant because the contrast factor of the organic polymer is insignificant.

Sample preparation and observation by cryogenic transmission electron microscopy, CryoTEM, were realized according to the following procedure. First, a (low viscosity) sample droplet was first placed on a carbon membrane grid and any excess of sample was quickly removed by a filter paper, leaving a thin film on the grid, then it was immediately quench-frozen in liquid ethane and cooled with liquid nitrogen. After verification that sample thickness was adequate, its observation was achieved with a LaB6 JEOL JEM2100 electron microscope.

The evolution of elastic and viscous moduli, G' and G" respectively, was measured as a function of temperature at a fixed shear frequency of 1 Hz, an applied strain of 0.2 %, and a heating/cooling rate of 1 °C/min. The measurements were carried out on a Physica RheoCompass rheometer by using a cone and plate geometry having a diameter = 50 mm and cone angle = 1° fitted with a solvent trap to minimize water evaporation. Birefringence of the samples was observed between cross-polarizers on samples previously heated to the measuring temperature.

We worked at a fixed molar ratio between laponite and F127 for which the copolymer does not form micelles. Instead, the macromolecules adsorb onto the laponite particles to produce hairy platelets as already shown in the past [23, 25, 26]. The adsorbed layer of copolymer has a thickness $\triangle e$ = 32 Å, which is assumed to be uniform on both the edge and sides of the nanoplatelets, and up to an adsorbed amount of 0.81 g of copolymer per g of nanoparticles at saturation (data shown

in supplemental material, figure S1). This thickness is mainly associated with the PEO blocks exposed to the solvent, while the PPO blocks are adsorbed directly onto the nanoparticles. Coating the nanoparticles with a polymeric shell has the additional effect to provide steric stabilization thus it avoids nanoparticles aggregation and ensure adequate phase equilibrium [27]. Overall, these characteristics lead to an effective thickness and diameter for the coated nanoplatelets of 73 and 344 Å respectively, giving a modified aspect ratio $l/d \sim 0.21$. In addition, the temperature dependence of the conformation of PEO chains in water allows the volume fraction of the coated nanoplatelets to vary with a minimal influence on the aspect ratio [28]. We therefore have two levers for studying the phase behavior of coated nanoplatelets in solution: by varying the concentration or the temperature. The results are discussed in the frame of existing theories and compared with the behavior of bare colloidal nanoplatelets in solution, having a lower aspect ratio $l/d \sim 0.03$.

Our main result is to show that the behavior of these somehow polydisperse coated nanoplatelets shows the emergence of a non-birefringent phase, composed of random stacks of nanoparticles as it is evidenced from structural techniques in a relatively low concentration range. These results are in line with most recent numerical predictions developed for (monodisperse) nanoplatelets [21, 29]. Additionally, we show that a transition from random stacks to nematic columnar order, i.e., nematic stacks, is easily triggered by an increase of temperature thanks to the thermosensitive nature of the PEO chains. As it could be anticipated, this structural transition is associated with a modification in both rheological and optical properties yielding highly viscoelastic and birefringent suspensions. We believe that these results, based on an easy-to-implement self-assembly process, open up a new route for the development of architecturally engineered nanocomposite from common polydisperse nanometric platelets.

We first studied the structure of both bare and copolymer coated nanoplatelets suspensions at room temperature as a function of concentration (ϕ = 1 wt. % $\rightarrow$ 14 wt. %), displayed on figure 1a and 1b respectively. For the sake of comparison with numerical data reported in the literature, these concentrations correspond to dimensionless number densities, $\rho^* = d^3 \times$number density, ranging from 0.14 to 2.2 for the bare nanoplatelets and from 0.44 to 6.8 for the coated nanoplatelets respectively. On the one hand, the scattering curves of bare laponite (figure 1a) display the characteristics known from previous studies [30-32]. At the lowest concentration, the scattering curves correspond to the theoretical form factor of polydisperse nanoplatelets, whereas at higher

concentrations two different regimes appear as a function of the wavevector q (figure S2). For $q \geq 2\pi/d$ (~ 0.02 $Å^{-1}$), experimental scattering data and theoretical form factor of polydisperse platelets overlap. For $q < 2\pi/d$, the scattered intensity, I(q), starts to decrease due to excluded volume interactions in agreement with data usually observed for laponite suspensions. We did not observe neither a correlation peak nor a permanent birefringence in this concentration range.

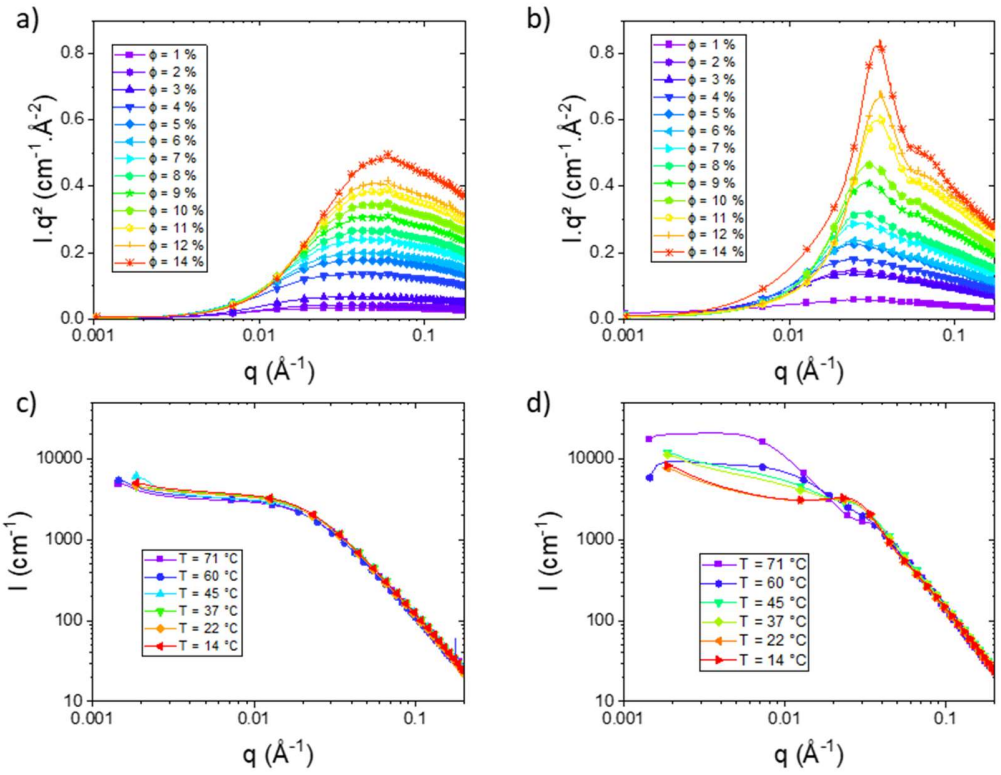

Figure 1. Scattering curves at room temperature for laponite concentrations (ϕ) ranging from 1 to 14 wt. % for bare laponite suspensions (a) and coated laponite suspensions (b). The figures (c) and (d) show scattering intensities at ϕ = 9 wt. % and T = 14, 22, 37, 45, 60 and 71°C for bare and coated laponite respectively.

On the other hand, while the scattering curves for coated laponite are similar to those observed for bare laponite at low concentrations, they become progressively different as the particle concentration increases (figure 1b). Thus, when $\phi \geq 2$ wt. %, the scattering curves of coated laponite show the progressive emergence of a structural peak located at q ~ 0.03 $Å^{-1}$. The amplitude of the peak increases with particle concentration, and a second order peak gradually emerges as shown on figure 1b and will be discussed later. The scattering data is drawn in Kratky representation

because when $q \geq 2\pi/d \sim 0.02$ Å^{-1}, the form factor decays as q^{-2} thus the factor $q^2 \times I(q)$ is proportional to the structure factor S(q) [33]. The position of the peak does not show significant shift when ϕ increases. It is worth adding that the sample viscosity sharply increases when $\phi \geq 13$ wt. %. Moreover, we did not notice any permanent birefringence of the samples (figure S5) though cryoTEM images clearly show the progressive stacking of nanoparticles as their concentration increases, as it can be seen on figure 2 where the nanoplatelets stacks of coated laponite are clearly visible. These results strongly indicate that the structural peak in I(q) is due to the progressive appearance of isotropic stacked platelets having a separation distance of ~ 200 Å.

As mentioned earlier, recent predictions have shown that the transition from I to random stacks prevails instead of a nematic mesophase. It is expected that when the Debye length is large and the average distance between particles decreases, it tends to reveal particle anisotropy and favors isotropic (or random) stacks [20]. This is because the repulsion is minimal for stacked configuration while it is maximum for side-to-side configurations, thus prompting the phase to evolve towards an isotropic distribution of short range stacked particles in full agreement with the present experimental observations [21].

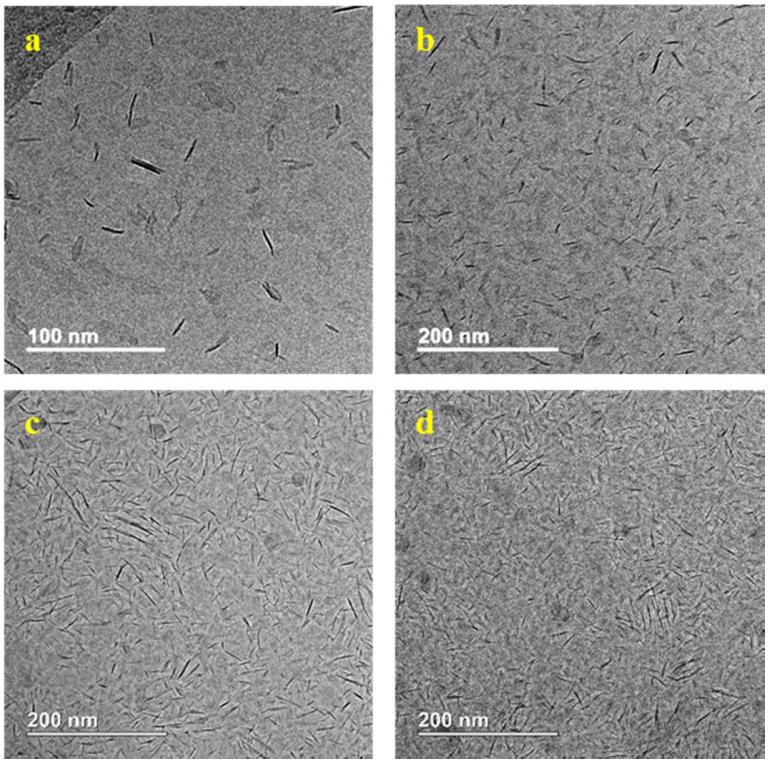

Figure 2. CryoTEM images at ϕ = 0.6 (a), 3 (b), 6 (c) and 9 wt. % (d), at room temperature.

We then investigated the behavior of our two systems as function of temperature in order to probe the contribution of the thermosensitive copolymer making up the shell of coated laponite. The grafted PEO blocks exposed to water are expected to show an increasing extension with increasing temperature, so that the effective volume fraction occupied by each hairy nanoparticle should increase [28]. Consequently, this thermally induced increase in volume fraction should make it possible to obtain highly oriented stacks (i.e. nematic stacks or nematic columnar mesophase), usually obtained by increasing particle concentration. The results are shown for the sample at ϕ = 9 wt. % for T ranging from 14 and 71°C (figure 1d), while, as it is expected, the behavior of bare laponite remains athermal (figure 1c). Let's first consider the case of coated particle data of figure 1d. For this system, two temperature domains can be distinguished. For T < 37°C, only the formerly observed correlation peak associated with stacking is present in SAXS data of coated nanoplatelets which is positioned at q ~ 0.03 $Å^{-1}$. Looking at the curves in more detail, one can see that the peak position shifts slightly with temperature, suggesting a decrease in the interparticle distance within the stacks.

When T increases above 40°C, the measurements show that a new order peak progressively appears and whose amplitude increases with T (ample data are displayed on figure S3 in supplemental material). It appears in the form of a shoulder at ϕ < 6 wt. % around q ~ 0.005 $Å^{-1}$. The appearance of this low q scattering peak strongly suggests that the suspensions evolve towards noticeable side-to-side positional ordering upon temperature increase as a result of intense excluded volume interactions.

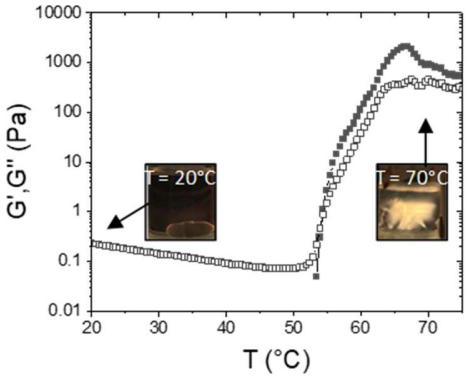

Figure 3. Evolution of elastic (G', solid symbols) and viscous (G'', open symbols) moduli as a function of temperature for suspension of coated nanoplatelets at ϕ = 9 wt. %. The inset images were taken between crossed polarizers at the different temperatures indicated in the figure.

Moreover, the previous experimental structural data are supported by additional results of the occurrence of the birefringence on the suspensions observed between cross-polarizers and by rheology measurements which are shown on figure 3 (and figures S5, S6 and S7). We should recall that at room temperature the suspensions of coated nanoplatelets with $\phi < 13$ wt. % are free flowing solutions, while they are highly viscous at 13 wt. % and viscoelastic at 14 wt. %. However, the observation between cross-polarizers, of the samples at room temperature, do not show detectable birefringence. When the temperature increases, both elastic and viscous moduli show a steep increase by many decades upon reaching a temperature threshold for all the samples when $\phi \geq 3$ wt. %. Above this span interval G' displays a light decrease while G" reaches a plateau. Inspection of the suspensions in the solidlike phase between cross-polarizers shows bright birefringent phases as it is displayed on the figure 3 for the sample at ϕ = 9 wt. %. These rheological behaviors are similar in many ways to the ones classically observed for micellar thermosensitive copolymer solutions as a function of temperature.

On the light of recently reported studies on nanoplatelets systems, such as the numerical calculations which investigated the phase behavior as a function of the charged nanoplatelets concentration and the range of the electrostatic potential [21], we rationalize our data as follows. First, in our experiments we explored the upper part of the phase diagram, where the electrostatic potential is screened, by varying the concentration between 1 and 14 wt. %, which corresponds to dimensionless number densities ρ^* varying from 0.44 to 6.8 for the coated nanoplatelets. Our results of the structural investigations show a succession of 3 phases. At concentrations < 2wt% ($\rho^* < 0.88$) the structure of the nanoplatelet suspensions corresponds to an isotropic phase which does not show the occurrence of any structural peak in SAXS intensity. Moreover, in this low concentration domain, the samples have low viscosities and remain non-birefringent. As the concentration increases above 2 wt. % ($\rho^* \geq 0.88$) the scattering intensities explicitly show the appearance of a structural peak, which we index as a 00l order peak located at $q \sim 0.03$ Å^{-1} and corresponds to a correlation distance of 200 Å, less than the nanoplatelet diameter. A second order correlation peak also appears for the concentrated samples. The data are shown in figure 4. All

these samples do not exhibit birefringence, which is in agreement with the results of cryoTEM. The latter clearly display the organization of nanoplatelets in stacks of a few nanoplatelets throughout the concentration range studied. No long-range orientation could be observed between the stacks, with some of them appear oriented parallel while others are perpendicular to the beam, in good agreement with the organization expected for the phase of random stacks predicted in the moderate concentration and high ionic strength domains, as it is the case in our experiments.

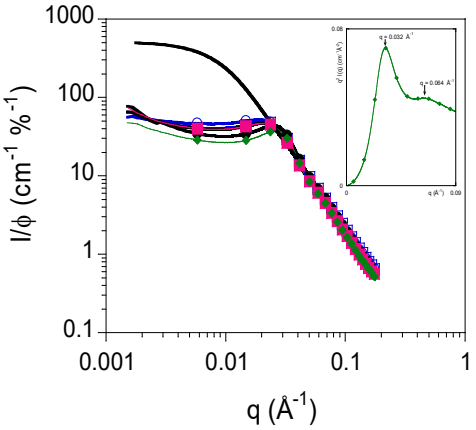

Figure 4. SAXS intensities normalized by the concentration for coated laponite at 6, 7, 8, 9, 10 and 11 wt. % and T = 22 °C (○, □, ◇, ●, ■ and ◆ respectively). (—) is the polydisperse form factor with d = 280 Å, l = 9.2 Å, polydispersity = 0.30. Inset: $q^2 \times I(q)$ (Kratky representation) at 11 wt. %.

We also mentioned that the nanoplatelets are functionalized using a grafting polymer which has the ability to stretch upon temperature increase [35, 36]. First, the correlation peaks that arise from particle stacking are still present as it is observed in the scattering spectra in figures 1 and 4. Moreover, above 50 °C, we observe 3 significant changes compared to the phase of random stacks. they consist of the appearance of a new structural peak localized in the low q value domain, ranging from 0.003 to 0.008 $Å^{-1}$, when the nanoplatelet concentration increases from 2 to 14 wt. % (ρ* ranging from 0.88 to 6.8). The occurrence of such low-q structural peak is associated with the emergence of strong birefringence and a steep increase of almost 5 orders of magnitude in the viscoelastic moduli. These characteristics are clearly the signature of a phase composed of oriented stacks or nematic stacks. The correlation peak corresponds to the average distance between the stacks, and whose position decreases from 2000 to 1000 Å when the concentration increases in the range investigated here. We also note that for this system made up of polydisperse nanoplatelets having a polydispersity index of 30%, only one single peak is visible. This observation is clearly in agreement with previous data which have shown that a large polydispersity index does not allow

the system to reach a high order organization such as a hexagonal crystal in this case. Actually, the structural studies of concentrated platelet suspensions made of gibbsite have shown that hexagonal packing of columns is triggered at high volume fractions, with successive secondary correlation peaks clearly visible in the spectra, but only when the polydispersity index is controlled below 25% [34].

In summary, we have studied the phase behavior, structure and rheology of suspensions of core/shell nanometric platelets, composed of an athermal mineral core and a thermo-responsive soft shell. We used aqueous suspensions of polydisperse laponite clay nanoparticles with a thermo-sensitive coating. The investigation shows that by tailoring the coating adequately, the small angle scattering of X-rays hints to the occurrence of randomly oriented stacks. The observation is in agreement with the data of cryoTEM which clearly display the organization of nanoplatelets in random stacks of a few nanoplatelets throughout the concentration range studied. When the temperature increases above a critical temperature, the shell of the adsorbed polymer increases in size and induces a phase transition from isotropically random stacks towards birefringent columnar phase formed by long range stacking of nanoplatelets, or so-called nematic stacks. The study of viscoelasticity shows a sharp increase of both moduli, as well as of the birefringence for the nematic stacks phase when the sample temperature decreases in this thermosensitive system. These findings are in agreement with the sequence of mesophases computed for platelets taking into account the anisotropy of the screened Coulomb potential. These results are an easy-to-implement process that could pave the way for the development of self-assembly of nanoplatelets at the nanoscale.

Acknowledgements

We thank Dr T. Bizien (Soleil Synchrotron) for his assistance with carrying out SAXS experiments on Swing beamline. Soleil synchrotron is gratefully acknowledged for beam time allocation.

Supplementary information

SI shows additional structural and rheology as well as birefringence images of the samples at extended concentrations.

References:

[1] Q. A. Akkerman, G. Rainò, M. V. Kovalenko, and L. Manna, Nat. Mater.,Genesis, challenges and opportunities for colloidal lead halide perovskite nanocrystals, 2018, **17**, 394-405.

[2] M. Ghidiu, M. R. Lukatskaya, M. Q. Zhao, Y. Gogotsi, and M. W. Barsoum, Nature, Conductive two-dimensional titanium carbide 'clay' with high volumetric capacitance, 2014, **516**, 78-81.

[3] M. Wei, F. P. G. de Arquer, G. Walters, Z. Yang, L. N. Quan, Y. Kim, R. Sabatini, R. Quintero-Bermudez, L. Gao, J. Z. Fan, F. Fan, A. Gold-Parker, M. F. Toney, and E. H. Sargent, Nat. Energy, Ultrafast narrowband exciton routing within layered perovskite nanoplatelets enables low-loss luminescent solar concentrators, 2019, **4**, 197-205.

[4] J. Di, J. Xiong, H. Li, and Z. Liu, Adv. Mater., Ultrathin 2D photocatalysts: electronic-structure tailoring, hybridization, and applications, 2018, **30**, 1704548.

[5] K. El Rifaii, H. H. Wensink, I. Dozov, T. Bizien, L. J. Michot, J. C. P. Gabriel, J. Breu, and P. Davidson, Langmuir, Do aqueous suspensions of smectite clays form a smectic liquid-crystalline phase?, 2022, **38**, 14563-14573.

[6] P. Davidson, C. Penisson, D. Constantin, and J. C. P. Gabriel, Proc. Nat. Acad. Sci., Isotropic, nematic, and lamellar phases in colloidal suspensions of nanosheets, 2018, **115**, 6662-6667.

[7] D. Monego, S. Dutta, D. Grossman, M. Krapez, P. Bauer, A. Hubley, J. Margueritat, B. Mahler, A. Widmer-Cooper, and B. Abécassis, Proc. Nat. Acad. Sci., Ligand-induced incompatible curvatures control ultrathin nanoplatelet polymorphism and chirality, 2024, **121**, e2316299121.

[8] L. Guillemeney, L. Lermusiaux, G. Landaburu, B. Wagnon, and B. Abécassis, Commun. Chem., Curvature and self-assembly of semi-conducting nanoplatelets, 2022, **5**, 7.

[9] D. Wang, M. Hermes, S. Najmr, N. Tasios, A. Grau-Carbonell, Y. Liu, S. Bals, M. Dijkstra, C. B. Murray, and A. van Blaaderen, Nat. Commun., Structural diversity in three-dimensional self-assembly of nanoplatelets by spherical confinement, 2022, **13**, 6001.

[10] A. K. Pearce, T. R. Wilks, M. C. Arno, and R. K. O'Reilly, Nat. Rev. Chem., Synthesis and applications of anisotropic nanoparticles with precisely defined dimensions, 2021, **5**, 21-45.

[11] I. Langmuir, J. Chem. Phys., The role of attractive and repulsive forces in the formation of tactoids, thixotropic gels, protein crystals and coacervates, 1938, **6**, 873-896.

[12] A. B. D. Brown, S. M. Clarke, and A. R. Rennie, Langmuir, Ordered phase of platelike particles in concentrated dispersions, 1998, **15**, 1594-1594.

[13] A. B. D. Brown, C. Ferrero, T. Narayanan, and A. R. Rennie, Eur. Phys. J. B, Phase separation and structure in a concentrated colloidal dispersion of uniform plates, 1999, **11**, 481-489.

[14] M. C. Mourad, D. V. Byelov, A. V. Petukhov, D. A. Matthijs de Winter, A. J. Verkleij, and H. N. W. Lekkerkerker, J. Phys. Chem. B, Sol − gel transitions and liquid crystal phase transitions in concentrated aqueous suspensions of colloidal gibbsite platelets, 2009, **113**, 11604-11613.

[15] H. N. W. Lekkerkerker, and G. J. Vroege, Phil. Trans. R. Soc. A, Liquid crystal phase transitions in suspensions of mineral colloids: new life from old roots, 2013, **371**, 20120263.

[16] A. V. Petukhov, J. M. Meijer, and G. J. Vroege, Curr. Opin. Colloid Interface Sci., Particle shape effects in colloidal crystals and colloidal liquid crystals: Small-angle X-ray scattering studies with microradian resolution, 2015, **20**, 272-281.

[17] J. A. C. Veerman, and D. Frenkel, Phys. Rev. A, Phase behavior of disklike hard-core mesogens, 1992, **45**, 5632.

[18] M. Marechal, A. Patti, M. Dennison, and M. Dijkstra, Phys. Rev. Lett., Frustration of the isotropic-columnar phase transition of colloidal hard platelets by a transient cubatic phase, 2012, **108**, 206101.

[19] Y. Ding, J. Yang, C. Wang, Z. Wang, J. Li, B. Hu, and C. Xia, Phys. Rev. Lett., Structural transformation between a nematic loose packing and a randomly stacked close packing of granular disks, 2023, **131**, 098202.

[20] S. Jabbari-Farouji, J. J. Weis, P. Davidson, P. Levitz, and E. Trizac, Sci. Rep., On phase behavior and dynamical signatures of charged colloidal platelets, 2013, **3**, 3559.

[21] S. Jabbari-Farouji, J. J. Weis, P. Davidson, P. Levitz, and E. Trizac, J. Chem. Phys., Interplay of anisotropy in shape and interactions in charged platelet suspensions, 2014, **141**, 224510.

[22] K. Mortensen, W. Batsberg, and S. Hvidt, Macromol., Effects of PEO− PPO diblock impurities on the cubic structure of aqueous PEO− PPO− PEO pluronics micelles: fcc and bcc ordered structures in F127, 2008, **41**, 1720-1727.

[23] I. Boucenna, L. Royon, P. Colinart, M. A. Guedeau-Boudeville, and A. Mourchid, Langmuir, Structure and thermorheology of concentrated pluronic copolymer micelles in the presence of laponite particles, 2010, **26**, 14430-14436.

[24] Y. Xu, W. J. Brittain, C. Xue, and R. K. Eby, Polymer, Effect of clay type on morphology and thermal stability of PMMA–clay nanocomposites prepared by heterocoagulation method, 2004, **45**, 3735-3746.

[25] I. Boucenna, L. Royon, M. A. Guedeau-Boudeville, and A. Mourchid, J. Rheol., Rheology and calorimetry of microtextured colloidal polycrystals with embedded laponite nanoparticles, 2017, **61**, 883-892.

[26] A. Nelson, and T. Cosgrove, Langmuir, Small-angle neutron scattering study of adsorbed pluronic tri-block copolymers on laponite, 2005, **21**, 9176-9182.

[27] P. Xu, Y. Lan, Z. Xing, and E. Eiser, Soft Matter, Liquid crystalline behaviour of self-assembled LAPONITE®/PLL–PEG nanocomposites, 2018, **14**, 2782-2788.

[28] I. W. Hamley, J. A. Pople, and O. Diat, Colloid Polym. Sci., A thermally induced transition from a body-centred to a face-centred cubic lattice in a diblock copolymer gel, 1998, **276**, 446-450.

[29] L. Morales-Anda, H. H. Wensink, A. Galindo, and A. Gil-Villegas, J. Chem. Phys., Anomalous columnar order of charged colloidal platelets, 2012, **136**, 034901.

[30] S. Bhatia, J. Barker, and A. Mourchid, Langmuir, Scattering of disklike particle suspensions: evidence for repulsive interactions and large length scale structure from static light scattering and ultra-small-angle neutron scattering, 2003, **19**, 532-535.

[31] A. Mourchid, E. Lecolier, H. Van Damme, and P. Levitz, Langmuir, On viscoelastic, birefringent, and swelling properties of laponite clay suspensions: Revisited phase diagram, 1998, **14**, 4718-4723.

[32] B. Ruzicka, E. Zaccarelli, L. Zulian, R. Angelini, M. Sztucki, A. Moussaïd, T. Narayanan, and F. Sciortino, Nat. Mater., Observation of empty liquids and equilibrium gels in a colloidal clay, 2011, **10**, 56-60.

[33] K. El Rifaii, H. H. Wensink, T. Bizien, J. C. P. Gabriel, L. Michot, and P. Davidson, Langmuir, Destabilization of the nematic phase of clay nanosheet suspensions by polymer adsorption, 2020, **36**, 12563-12571.

[34] F. M. Van der Kooij, K. Kassapidou, and H. N. W. Lekkerkerker, Nature, Liquid crystal phase transitions in suspensions of polydisperse plate-like particles, 2000, **406**, 868-871.

[35] K. Mortensen, and W. Y. N. Brown, Macromolecules, Poly (ethylene oxide)-poly (propylene oxide)-poly (ethylene oxide) triblock copolymers in aqueous solution. The influence of relative block size, 1993, **26**, 4128-4135.

[36] K. Mortensen, and Y. Talmon, Macromolecules, Cryo-TEM and SANS microstructural study of pluronic polymer solutions, 1995, 28, 8829-8834.